Petrologic Characteristics of Cenozoic Alkaline Basalts from the Azas Plateau, Northeast Tuva (Russia)

Yury LITASOV[1,2], Toshiaki HASENAKA[2], Konstantin LITASOV[3], Vladimir YARMOLYUK[4], Amina SUGORAKOVA[5], Vladimir LEBEDEV[5], Minoru SASAKI[6], Hiromitsu TANIGUCHI[3]

Keywords: Alkaline basalt, Cenozoic volcanism, Plateau lava, Baikal Rift

Abstract

The Azas Plateau is a part of the East-Tuva Highland (West Sayan ridge, the south of Krasnoyarsk Region, Siberia). It is the westernmost lava field of the Baikal Rift System, covering about 2000 km^2. A volume of volcanics is estimated as high as 600 km^3. The volcanics are represented by massive lava flows and thick hyaloclastite units. Their composition corresponds to alkaline basalts and basanites.

The most intensive volcanic activity started about 2 Ma from basaltic fissure eruptions producing voluminous lava flows. The second stage voluminous eruptions formed the upper lava unit on the surface of moderately eroded lower lava flows. During the next stages, the eruptions became centralized so that several volcanic centers were formed along certain lineaments marking deep-seated fissures. The peculiarity of the volcanic activity is that at least 7 volcanoes were formed during extensive glaciation covering the entire area of plateau. Moreover, the subglacial eruptions occurred about 0.7 and 0.1 Ma ago, whereas there was no sign of glaciation about 0.29 Ma ago, when Yurdawa shield volcano erupted. The subglacial eruptions formed table mountains (tuyas) with resembling structure of thick lower hyaloclastite units and armoring upper lava flows.

The composition of lavas is rather uniform with slight variations in acidity and alkalinity of volcanics during eruptions. The most voluminous eruptions produced trachy-basalts, smaller volcanoes are composed of tephrites/basanites. The basalts have typical for silica undersaturated rocks normalized REE patterns with regular enrichment in LREE and depletion in HREE. REE patterns, in accordance with eruption volumes, show lower degrees

1 Institute of Geology, United Institute of Geology, Geophysics and Mineralogy, Russian Academy of Sciences, Siberian Branch, Novosibirsk
2 Research Institute of Materials and Resources, Faculty of Engineering and Resource Science, Akita University
3 Center for Northeast Asian Studies, Tohoku University
4 Institute of Geology of Ore Deposits, Petrography, Mineralogy and Geochemistry, Russian Academy of Sciences, Moscow
5 Tuvinian Institute for the Exploration of Natural Resources, Russian Academy of Sciences, Siberian Branch, Kyzyl
6 Department of Earth and Environmental Sciences, Faculty of Science and Technology, Hirosaki University

of partial melting for tephritic volcanoes (La/Yb=12-17) and higher degrees for trachy-basalts (La/Yb=5-9). Correlation between La/Yb and Mg# indicates the formation of basalts by chemically identical source with one definite exception (Yurdawa volcano). The trace element compositions plotted on chondrite-normalized spidergram have OIB-like patterns.

1. Introduction

The Central Asia is a region of the Cenozoic volcanism associated with continental rift systems, and contains lava plateaus, discrete central and composite volcanoes, and lava flows [Whitford-Stark 1983: 193-222]. Within the Baikal Rift System, volcanic activity started from the Oligocene, and culminated in the Miocene. A few regions remained active until the Holocene. The youngest radiogenic ages of 0.002 Ma were reported from Uchuchei, Kislyi Klyuch, and Inarichi volcanoes, Udokan Plateau [Devirts et al. 1981: 1250-1253; Stupak, 1987: 88]. Several cones from the Tunka valley and East Sayan were assumed to be of Holocene age from topography [Adamovich et al. 1959: 88]. Scientific writings, however, rarely mentioned Central Asia as an area of active volcanoes due to lack of appropriate information. Recent publications show that the volcanism there is characterized by short-term activities separated by much longer periods of dormancy, which exceeds the extent of human history [Yarmolyuk et al. 1999: 244-249; 2001: 3-32].

Terrestrial alkaline basalts occur in different tectonic settings. Dominant are continental rift zones and oceanic and continental hot spots, with some unique exceptions including alkaline basalts on ocean-ward slope toe of the Japan Trench [Hirano 2000: 254]. Alkaline basalt feeding dykes and lava flow fragments were reported from Inner Asia active orogenic belt including Tien Shan, Pamir and Tibet [Dobretsov et al. 1977: 648-651; Baratov et al. 1988: 702-706; Lutkov, 1988]. Within the rift zones, alkaline volcanism often concentrates beyond main rift depressions, above lithospheric slopes, or at the ends of rift structures, within areas where rifting events are not pronounced clearly. Two contrasting mechanisms of alkaline basalt formation are identified from various settings, which are a decompressional melting (for example, alkaline basalts of the Antarctic Peninsula [Hole et al. 1993: 51-68]) and mantle plume activity (Hawaiian hot spot [Chen et al. 1990: 197-218]). Both mechanisms were described for the formation of alkaline basalts in continental rift settings [Yarmolyuk and Kovalenko 1990: 187-191; Keen et al. 1994: 403-416; Zhang and O'Reilly 1997: 33-54].

The Tuva volcanic province corresponds to the westernmost branch of the Baikal Rift System (Fig.1). This paper is dedicated to petrology of Azas alkaline basalts and problem of their origin.

Obruchev [1949; 1950] performed first studies in this area. He divided the volcanic sequence into three major units - lower lavas (Pliocene), middle tuff layers (Late Pliocene-Early Pleistocene) and upper lava flows (Middle Pleistocene). Small scoria cones were interpreted as the Holocene volcanic products. Similar results were presented from the

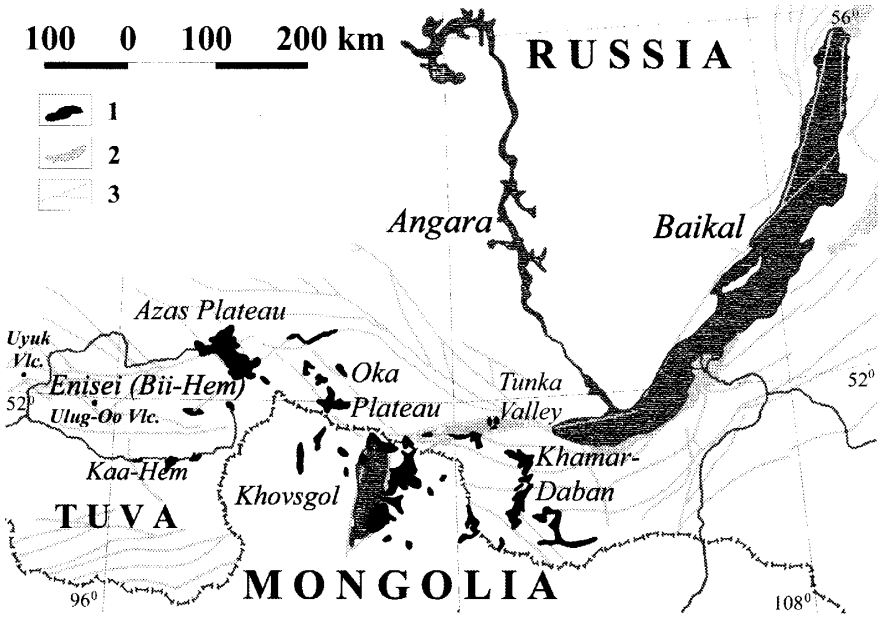

Fig.1. Schematic map of the southwestern Baikal Rift System. Legend: 1 - volcanic fields; 2 - sedimentary basins (rift depressions) ; 3 - major faults.

1:200,000 state geological survey mapping work. The age estimations were based mostly on the geomorphologic data.

During the last few years, we studied the volcanic rocks of the Azas Plateau and several other localities of Cenozoic alkaline basalts in northeastern Tuva. Our new data allowed significant evaluation of volcanic events. Precise age determinations changed our view on the Cenozoic volcanism within the Baikal Rift System. New geochemical data provided better understanding of alkaline basalt formation mechanism.

2. Geological and tectonic background

The Baikal Rift opening started from 70 to 30 Ma ago [Logachev and Zorin 1987: 225-234; Rasskazov et al. 1994: 949-654]. Two segments with different tectonic history are identified. Northern Baikal Rift developed as amagmatic depressions and volcanic fields shifted to the southeast-south from the rift axis (Tokinskii Stanovik Ridge, Udokan Plateau, Vitim Plateau). Southern Baikal Rift includes graben depressions with moderately developed volcanism and lava fields to the south and west (Tunka Valley, Hamar-Daban Ridge, Dzhida and Bartoi River Basins, Khovsgol Lake Basin, Oka Plateau, and Azas Plateau). The triple junction of rift-related valleys was interpreted as the South Baikal hot spot [Yarmolyuk and Kovalenko 1990: 187-191]. The mantle plume activity there forced the domal uplift with highest altitudes above 3000 m a.s.l. (Mt. Munku-Sardyk) at the triple junction of Khovsgol Basin, Tunka Depression, and Oka-Azas troughs. The last have less pronounced rifting tectonics. However, the volcanism at the Oka-Azas region started from the early stage of Baikal Rift formation as small volcanoes and continued later with formation of extended lava plateaus.

The development of Azas Plateau as compared to the closest Oka Plateau reveals

centrifugal character of volcanism along troughs (Fig. 1). The most voluminous volcanism of Oka basin and formation of lava plateau started from the Late Oligocene. Within Tuva, only small monogenetic volcanoes formed. In the Early-Middle Miocene, the Oka trough and contemporaneous 200-300 m thick lava field were formed. Outside the trough, the fissure eruptions occurred in the Northeast Tuva forming valley-filling lava flows. The formation of Oka trough ended in the Middle Miocene; however the uplift of the entire region continued, so the river valleys cut deep into Oka lava plateau. Those valleys became depositional sites of lavas for the Late Miocene and Pliocene volcanic eruptions. The Miocene-Pliocene formation of the Azas trough was not accompanied by volcanism. The Late Pliocene eruptions occurred on the surface of the existing Azas trough, and formed the Azas lava plateau. From the Late Pliocene, the main volcanic activity shifted from the Oka basin to the Azas trough and continued in this area until the Holocene. Both troughs elongated in the northwest direction, however the Azas trough shifted southwest relative to the Oka trough along the northeast-oriented fault, which becomes the major lineament controlling the site of volcanism.

The Tuva volcanic province includes numerous localities of the Cenozoic volcanism. The lava flow fragments are found along the upper stretches of the Enisei River, and their stratigraphy reveals multi-stage volcanic activity. For instance, the basalt lavas occur on

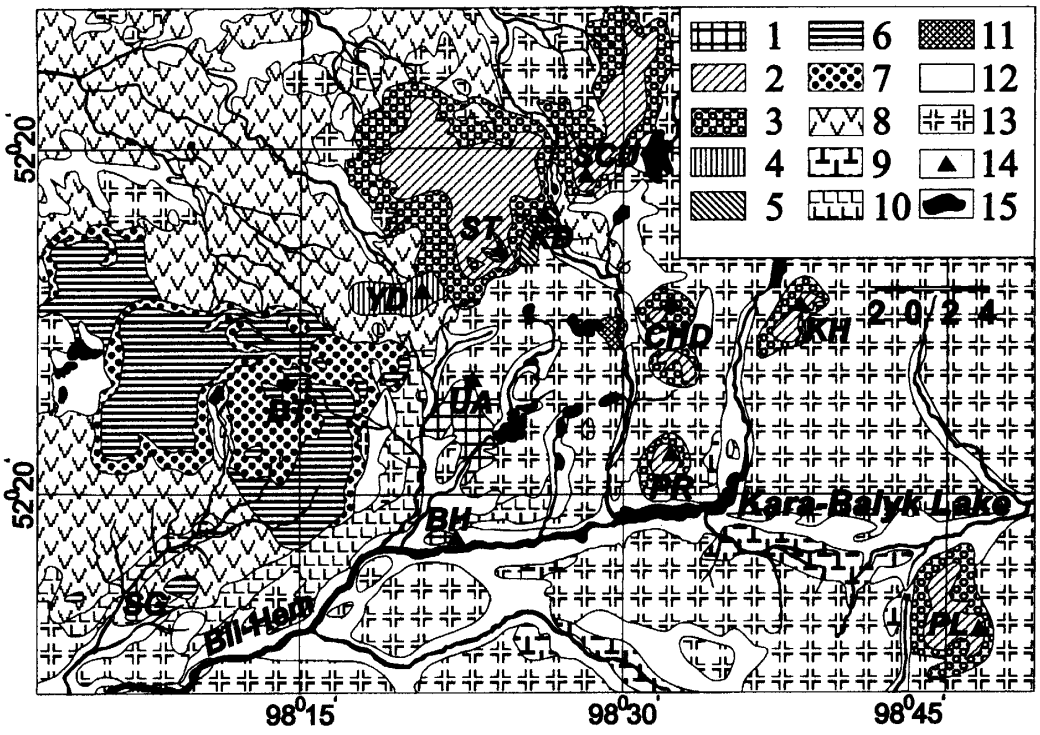

Fig.2. Southeastern part of the Azas Plateau. Legend: 1 - Holocene-0.05Ma lava flows; 2-3 - 0.075-0.225Ma volcanics (2 - lava flows; 3 - hyaloclastites); 4 - 0.29-0.35Ma lava flows; 5 - 0.56-0.60Ma lava flows; 6-7 - 0.725-0.76Ma volcanics (6 - lava flows; 7 - hyaloclastites); 8 - 1.2Ma lava flows; 9 - 1.65-1.75Ma lava flows; 10 - 2.1Ma lava flows; 11 - 14.7Ma lava flows; 12 - morains and alluvial deposits; 13 - basement; 14 - volcanic centers; 15 - water reservoirs. Volcanoes: BH - Bii-Hemskii; UA - Ulug-Arginskii; PL - Ploskii; PR - Priozernyi; KH - Kok-Hemskii; CHD - Charash-Dag; SCU - Sorug-Chushku-Uzu; ST - Shivit-Taiga; YD - Yurdawa; KD - Kadyr-Sugskii; SG - Sagan; DT - Derbi-Taiga.

different levels of terraces along the river valleys, compose discrete volcanoes and extended lava plateaus. The largest is the Azas Plateau located between Hamsara and Bii-Hem (Bolshoi Enisei) rivers and controlled by the Azas depression (Fig. 2). It covers 2400 km^2 and the volume of volcanic products is estimated to be 600 km^3 [Yarmolyuk et al. 1999: 244-249; Rasskazov et al. 2000: 655-659].

The volcanism appeared as pulses. At least 9 stages of volcanism are found during the last 2.5 Ma. Shield volcanoes were formed by Hawaiian-type basaltic fissure eruptions, with the presence of small scoria cones limited to the feeding centers representing the explosive activity. Estimation of eruption volume is difficult, because of significant erosion by contemporaneous or later glaciers. Two stages coincided with widespread glaciation of the region; subglacial eruptions of Icelandic-type created table mountains with 400-500 m thick hyaloclastites and upper armoring massive lava flows.

3. Sequence of volcanism stages

The oldest volcanoes of the Tuva volcanic province are located outside Azas Plateau; they compose discrete volcanic centers to the west and southwest from the plateau. Among them, the Uyuk volcano is 28 Ma old, and Ulug-Oo volcano is 23 Ma old [Yarmolyuk et al. 1999: 244-249; Sugorakova, personal communication]. Probably, the basalt lavas from high terraces along Kaa-Hem and Bii-Hem rivers belong to this stage because of their resemblance in chemical composition and geomorphologic peculiarities (located 200-300 m above the river bed).

Only fragments of lava flows in the basin of Kadyr-Sug River and high terraces to the northwest of lava plateau (Ulug-Arga Ridge) represent the Middle Miocene stage. Reported ages are 16 to 14.7 Ma [Rasskazov et al. 1989: 77-85; Yarmolyuk et al. 1999: 244-249]. Their location at different hypsometric levels suggests the formation of the Azas trough after the Middle Miocene. The present thickness exceeds 100 m in local depressions.

The Late Pliocene stage (2.1 Ma) is characterized by the most voluminous eruptions, which generally formed the lava plateau within the Azas trough. The plateau has gently inclined surface with decreasing altitudes from 2200 m at the southeast to 1200 m at the northwest between the 70 km distance. The lava flows smoothed mountainous relief; their total thickness is variable with the estimated average of about 250 m.

The Early Pleistocene volcanic activity is divided into two stages. The lava flow fragments on the upper terraces of Bii-Hem River and a watershed between Tissa, Bilin and Bii-Hem rivers have ages 1.65-1.75 Ma. These flows extend along paleovalleys on the surface of eroded Late Pliocene lava plateau and adjacent exposures of basement. 100-200 m thick lava flows between Shivit-Taiga and Derbi-Taiga volcanoes have ages about 1.2 Ma and compose the upper plateau; their northwest extension was not examined.

During the Late Pleistocene, the Derbi-Taiga volcano was formed (0.725-0.76 Ma). In earlier studies, its huge middle portion of volcanoclastic strata was described as volcanic tuffs [Grosvald et al. 1959: 91-104]. However, the presence of various glassy fragments,

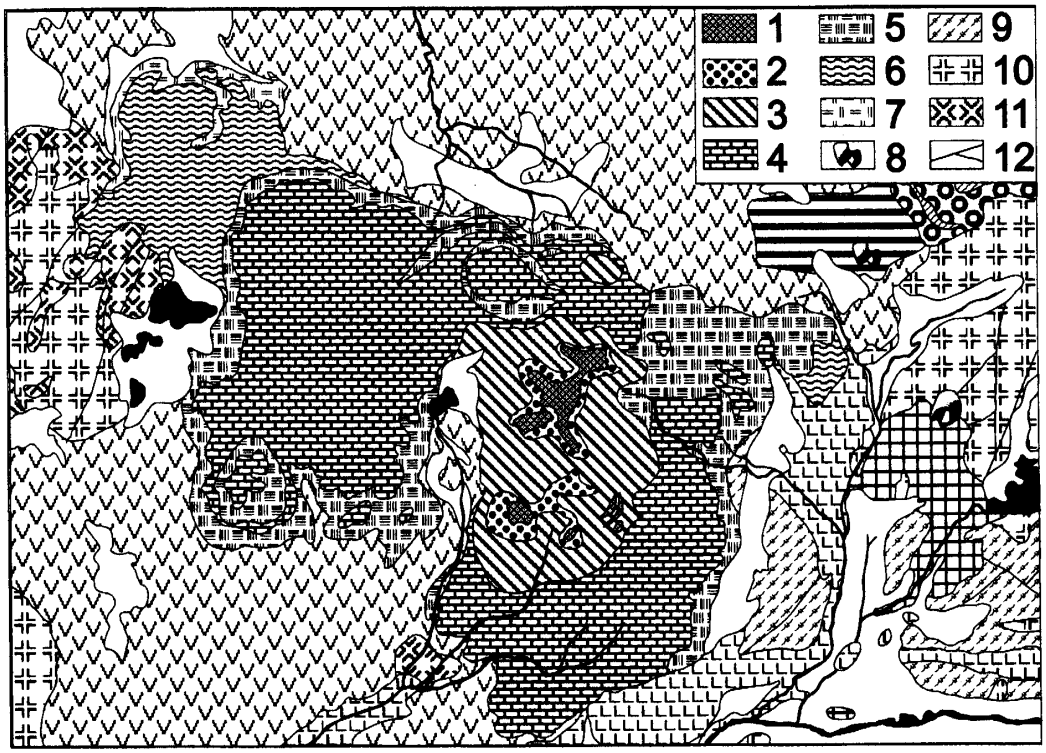

Fig.3. Structure of Derbi-Taiga Volcano. 1 - Upper armoring lava flows; 2 - pillow lavas; 3 - upper hyaloclastites; 4 - middle lava flows; 5 - middle hyaloclastites; 6 - lower lava flows; 7 - lower hyaloclastites; 8 - scoria cones of Yurdawa and Ulug-Arginskii volcanoes; 9 - 10 - 11 - 12 - major faults. Other symbols as in Fig.2.

mode of matrix alteration (fine and glassy material, chlorite, and palagonite), upward appearance of pillow lavas allowed consideration of these rocks as hyaloclastites (Fig. 3). We made a scenario of the formation of volcano during increasing glaciation, because of the distribution of lava flows and hyaloclastites. First, it was developed as normal shield stratovolcano with 10-20 m thick hyaloclastites (initial stage of glaciation) lying at the base and up to 100-m thick massive lavas. Some 20-30 m thick overlying hyaloclastites and 50-150 m thick massive lavas characterize the next eruption. Finally, the 400-550 m thick layer of hyaloclastites developed after the formation of glacier. When the extruding lava reached the surface of glacier, the 30-70 m thick massive lava flows were formed protecting lower layers from erosion. Locally, feeding dykes and necks were found in the body of hyaloclastites.

From 0.6 to 0.29 Ma, three small volcanoes formed around Derbi-Taiga. Their lava shields do not exceed 100 m of total thickness. The Kadyr-Sugskii volcano (0.6-0.56 Ma) is partly exposed southeast of the Shivit-Taiga volcano, the Yurdawa volcano (0.35-0.29 Ma) is located between the Derbi- Taiga and Shivit-Taiga, and the Sagan volcano takes place south of the Derbi-Taiga. Volcanic products from the Kadyr-Sugskii and Yurdawa volcanoes bear numerous mantle xenoliths and cumulates.

Toward the end of Late Pleistocene (0.225-0.075 Ma), several shield volcanoes of different size formed at the eastern extent of the Azas plateau. Their table mountains are

towering on the surface of Late Pliocene lavas and Proterozoic basement rocks. The largest are Shivit-Taiga and Sorug-Chushku-Uzu volcanoes; others include Charash-Dag, Kok-Hemskii (Fig. 4a,b), Priozernyi and Ploskii volcanoes. Their structures resemble, but are simpler than one of the Derbi-Taiga, because they have been formed during intensive glaciation of the entire region and do not have lower massive lavas. They contain lower 250-500 m thick hyaloclastite unit, upper armoring 50-100 m thick massive lava flows, and, in most cases, small scoria cone as the highest point on the surface of relatively flat summits. The rock fragments in friable material of hyaloclastite increase in size upwards, where the pillow-lavas underlie the upper massive lava flows.

At the end of Late Pleistocene, the Ulug-Arginskii volcano formed (0.05 Ma). It is located on the slope of Ulug-Arga Mount (Fig. 4c), and is composed of well-preserved scoria cone and adjacent lava flows up to 50 m in total thickness. Another possible Holocene locality was found in 1999; well-preserved lava flows near the bed of Bii-Hem River, however radiogenic age determination has not been performed.

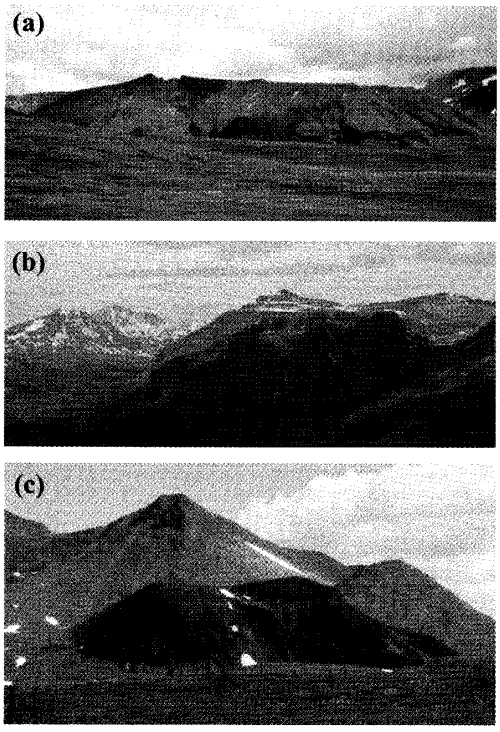

Fig.4. Volcanoes of the Azas Plateau: a,b - Kok-Hemskii Volcano table mountain (a - western view; b - southern view) ; c - Ulug-Arginskii Volcano scoria cone.

4. Petrography of volcanic rocks

Hyaloclastites form as the result of the eruption of massive lavas into glacier body, as it has been described for the Island volcanoes. Therefore, the amount of lavas multiplies that of pyroclastic materials, which are concentrated in relatively small scoria cones. The lava composition is relatively uniform and dominated by alkaline basalts (trachybasalts) and basanites-tephrites (Fig. 5). Their textures are also uniform; the rocks are represented mostly by aphyric varieties containing variable amounts of olivine and sometimes Ti-augite

Table 1. Modal analyses of lavas from Azas Plateau compared with norm values

Location		Bii-Hemskii (2)		Priozernyi (4)		Priozernyi (4)		Shivit-Taiga (5)		Kok-Hemskii (6)		Charash-Dag (7)	
Sample No		BH-1		PR-1		PR-3		ST-1		KH-2		CHD-1	
Age (Ma)		*Holocene*		*0.075*		*0.075*		*0,11-0,13*		*0.15*		*0.21*	
Rock type		*trachybasalt*		*basanite*		*basanite*		*trachybasalt*		*trachybasalt*		*basanite*	
modal	norm	modal	norm	modal	norm	modal	norm	modal	norm	modal	norm	modal	norm
Alk Fsp	Or	3.9	8.87	1.1	12.66	3.2	12.09	1.6	9.12	2.8	12.95	1.5	14.24
	Ab		27.10		20.38		21.20		25.62		28.15		15.33
	An		18.19		15.85		15.70		18.34		19.89		14.93
Pl	Norm Pl	41.1	45.30	38.2	36.23	37.1	36.90	34.6	43.96	40.7	48.04	30.3	30.26
Ne	Ne		4.44		9.51	tr	9.60	tr	4.64	tr	4.06	tr	9.47
Cpx	Di	10.8	15.58	10.5	15.60	15.5	15.81	1.3	15.03	12.0	13.17	13.7	15.42
Ol	Ol	11.3	17.95	11.8	17.51	10.6	17.04	2.3	18.46	5.4	13.56	18.1	21.41
	Mt		2.64		2.53		2.53		2.72		2.27		2.55
	Ilm		4.06		4.36		4.42		4.70		4.39		4.69
Ore	Mt+Ilm	8.4	6.71	8.1	6.89	7.7	6.95	1.3	7.42	0.6	6.65	5.6	7.24
Ap	Ap		1.16		1.60		1.61		1.36		1.57		1.97
Gl+fine		24.5		30.3		25.9		58.9		38.5		30.8	
	Total	100.0	100.00	100.0	100.00	100.0	100.00	100.0	100.00	100.0	100.00	100.0	100.00

Location		Ploskii (8)		Ploskii (8)		Kadyr-Sug (10)		Derbi-Taiga (11)		Kaa-Hem (13)		Kaa-Hem (13)	
Sample No		PL-2		PL-3		KD-1		DB-4		SB01		SB03	
Age (Ma)		*0.225*		*0.225*		*0,56-0,60*		*0,725-0,76*					
Rock type		*trachybasalt*		*trachybasalt*		*basanite*		*basanite*		*trachybasalt*		*trachybasalt*	
modal	norm	modal	norm	modal	norm	modal	norm	modal	norm	modal	norm	modal	norm
Alk Fsp	Or	5.9	11.05	11.1	13.00	10.4	12.21	1.7	12.87		9.54		9.17
	Ab		28.27		27.54		17.12		15.48		25.42		24.68
	An		19.92		18.67		16.25		16.65		20.94		18.27
Pl	Norm Pl	48.0	48.19	45.5	46.21	28.6	33.37	14.5	32.13	41.9	46.36	31.8	42.95
Ne	Ne		1.50		5.76	tr	9.27	0.9	9.82		1.86		4.99
Cpx	Di	10.1	14.10	12.0	14.00	10.7	16.81	17.5	20.62	13.1	14.71	6.3	15.50
Ol	Ol	13.3	17.45	11.4	12.74	16.0	19.38	2.7	15.32	17.7	18.83	10.1	18.58
	Mt		2.41		2.30		2.68		2.48		2.67		2.71
	Ilm		4.03		4.46		4.74		4.89		4.62		4.66
Ore	Mt+Ilm	6.9	6.44	7.1	6.76	6.3	7.42	6.2	7.37	7.9	7.29	5.8	7.37
Ap	Ap		1.28		1.53		1.54		1.87		1.41	tr	1.43
Gl+fine		15.8		12.9		28.0		56.5		19.4		46.0	
	Total	100.0	100.00	100.0	100.00	100.0	100.00	100.0	100.00	100.0	100.00	100.0	100.00

Location		Lower plateau (15)		Shui flows (16)		Shui flows (16)		Ulug-Oo (17)		Ulug-Oo (17)		Uyukskii (18)	
Sample No		LP-1		SB04		SB06		SB11		SB15		UY-1	
Age (Ma)		*1,73-2,14*						*23*		*23*		*28*	
Rock type		*trachybasalt*		*trachybasalt*		*phonotephrite*		*phonotephrite*		*tephrite*		*phonotephrite*	
modal	norm	modal	norm	modal	norm	modal	norm	modal	norm	modal	norm	modal	norm
Alk Fsp	Or	tr	9.11	tr	18.95	1.9	20.93	4.9	17.35	3.5	22.26	15.3	16.07
	Ab		21.97		23.62		28.14		23.22		14.38		35.38
	An		18.92		17.14		9.33		10.65		6.60		11.58
Pl	Norm Pl	40.1	42.64	35.8	40.76	36.9	37.47	20.9	33.87	16.5	20.98	20.6	46.96
Ne	Ne		2.09		2.85	tr	9.72		10.15	tr	16.29		5.84
Cpx	Di	13.5	15.91	12.4	12.50	10.7	12.09	11.7	13.87	9.5	12.27	11.3	10.24
Ol	Ol	23.1	23.20	14.2	16.39	11.2	11.52	14.5	15.20	11.7	16.56	11.2	13.34
	Mt		2.88		2.24		2.05		2.22		2.34		1.87
	Ilm		4.78		4.40		3.87		4.22		4.99		3.61
Ore	Mt+Ilm	6.5	7.66	5.1	6.63	6.5	5.92	6.9	6.43	7.1	7.33	5.5	5.48
Ap	Ap		1.15		1.92		2.37		3.13		4.32		2.07
Gl+fine		16.8		32.5		32.8		41.1		52.7		36.1	
	Total	100.0	100.00	100.0	100.00	100.0	100.00	100.0	100.00	101.0	100.00	100.0	100.00

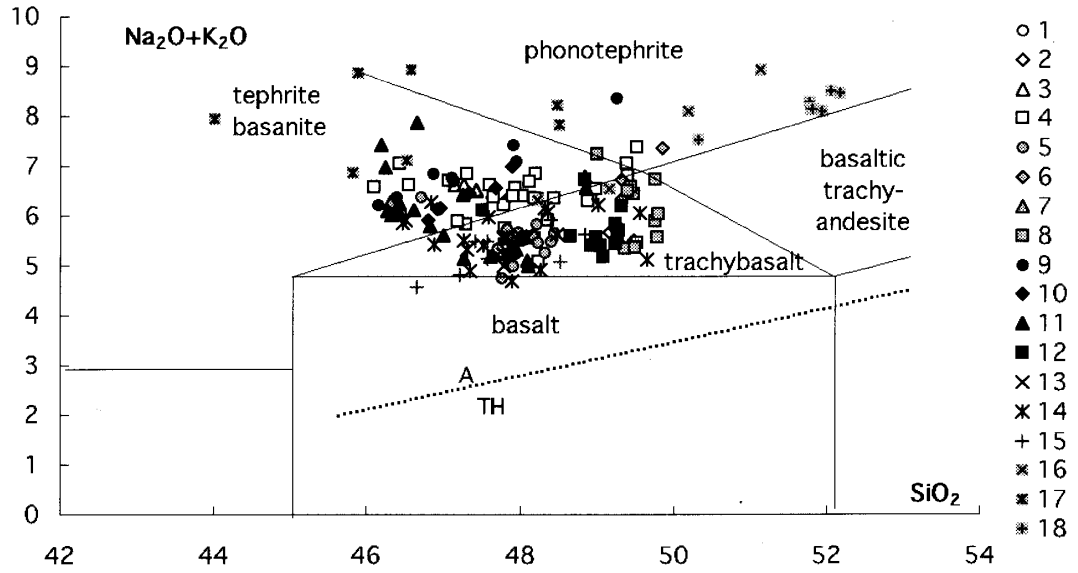

Fig.5. TAS diagram for the Tuvinian Cenozoic basalts. Symbols: 1 - Ulug-Arginskii Vlc.; 2 - Bii-Hemskii Vlc.; 3 - Sorug-Chushku-Uzu Vlc.; 4 - Priozernyi Vlc.; 5 - Shivit-Taiga Vlc.; 6 - Kok-Hemskii Vlc.; 7 - Charash-Dag Vlc.; 8 - Ploskii Vlc.; 9 - Yurdawa Vlc.; 10 - Kadyr-Sugskii Vlc.; 11 - Derbi-Taiga Vlc.; 12 - lava flow fragments on the terraces of Bii-Hem River; 13 - lava flows on the 2nd terrace of Kaa-Hem River; 14 - Upper Plateau lava flows; 15 - Lower Plateau lava flows; 16 - lava flow fragments on the higher terraces of Kaa-Hem River; 17 - Ulug-Oo Vlc.; 18 - Uyukskii Vlc.

(Derbi-Taiga) phenocrysts. Matrix is composed of dominant plagioclase microlites with variable amount of clinopyroxene, olivine and Ti-magnetite. Interstitial space is composed of plagioclase and alkali feldspars surrounded by cryptocrystalline or glassy material. The amount of alkali feldspars increases in basanites and tephrites; fine-grained nepheline crystals appear in highly alkaline varieties. The basalt fragments in hyaloclastites, especially their outer zones, are composed of dark glassy material with olivine phenocrysts, small Ti-augite and plagioclase microlites. The modal contents obtained by point counting are less than respective norm values (Table 1), because of large amount of glassy or fine-grained materials.

5. Chemical compositions

Major and some trace element compositions of bulk rocks were measured using Philips XRF PW2400 at Hirosaki University. Detailed measurement conditions are described in Sasaki [1999: 141-149]. REE's (rare earth elements), Th, Nb, Y, and some other trace elements were determined by using VG Elemental ICP-MS PQ3 at Akita University. Detailed descriptions of analytical procedures appear in Satoh et al. [1999: 1-8].

Major element compositions are listed in Table 2. SiO_2 contents range from 44 to 52 wt% (Fig. 5), and Na_2O+K_2O from 4.5 to 9 wt%. These rocks on the TAS diagram plot to the fields of trachybasalts, basanites-tephrites, phonotephrites, and basaltic trachyandesites. The first two comprise a majority of rock types. The age and rock compositions do not correlate clearly. However, conformity was found between approximate volume of erupted material and rock alkalinity. For instance, the basalts of voluminous lower and upper

Table 2. Major element analyses of lavas from Azas Plateau

Locality	2	1	1	4	5	5	6	7	8	9	10	11	11
Sample No	BH-2	UA-1	UA-2	PR-2	ST-5	ST-6	KH-3	CHD-1	PL-2	YD-1	KD-1	DB-2	DB-4
Age (Ma)	Holocene	0.048	0.048	0.075	0.11	0.11	0.15	0.21	0.225	0.29	0.56	0.725	0.725
Rock type	BSN	BSN	BSN	BSN	TRB	TRB	PHT	BSN	TRB	PHT	BSN	TPH	BSN
SiO_2	47.82	45.42	46.43	48.21	48.45	47.80	49.86	46.31	49.79	49.26	46.97	46.66	46.62
TiO_2	2.53	2.83	2.89	2.37	2.42	2.44	2.35	2.46	2.12	2.76	2.51	2.70	2.56
Al_2O_3	15.37	14.87	15.18	15.98	15.27	14.94	16.99	14.40	15.38	16.25	14.93	16.91	14.90
Fe_2O_3	12.47	12.64	12.70	11.37	12.57	12.39	10.00	11.69	11.11	11.70	12.40	11.11	11.34
MnO	0.16	0.16	0.16	0.15	0.16	0.16	0.14	0.15	0.15	0.13	0.16	0.15	0.16
MgO	7.61	7.74	7.78	6.71	7.67	7.53	4.50	9.56	7.27	5.00	8.44	4.93	7.44
CaO	8.16	8.11	8.18	7.77	8.31	8.41	7.88	7.92	8.23	6.14	8.35	7.88	9.45
Na_2O	4.48	4.42	4.41	4.72	4.08	3.75	4.91	3.86	3.67	5.09	4.07	5.24	3.95
K_2O	1.82	2.09	2.17	2.12	1.55	1.46	2.45	2.40	1.87	3.26	2.08	2.61	2.16
P_2O_5	0.66	0.72	0.74	0.74	0.57	0.58	0.74	0.85	0.55	0.80	0.67	0.94	0.80
Total	101.07	99.00	100.64	100.15	101.05	99.45	99.82	99.60	100.15	100.39	100.57	99.14	99.37
Na_2O+K_2O	6.30	6.51	6.58	6.85	5.63	5.21	7.35	6.26	5.55	8.35	6.15	7.85	6.11

Locality	15	15	13	14	14	14	14	14	15	16	17	17	18
Sample No	BH-3	BH-4	SB02	UP-1	UP-2	UP-3	UP-4	UP-5	LP-1	SB08	SB13	SB16	SB17
Age (Ma)	2.1	2.1		1.65	1.65	1.65	1.65	1.65	1.73	23	23	23	28
Rock type	TRB	TRB	TRB	BSN	TRB	TRB	TRB	TRB	TRB	BSN	PHT	PHT	PHT
SiO_2	48.66	49.25	48.01	46.51	47.90	47.86	49.56	48.49	50.50	48.23	48.48	46.58	52.18
TiO_2	2.22	2.10	2.45	2.74	2.60	2.69	2.95	2.56	2.51	2.37	2.21	2.55	1.88
Al_2O_3	15.27	15.31	14.99	15.15	14.67	15.06	15.79	15.25	14.75	14.86	15.14	14.69	16.10
Fe_2O_3	12.21	12.29	12.41	12.92	11.83	13.14	12.06	12.96	12.75	10.71	9.93	11.10	8.53
MnO	0.16	0.16	0.16	0.16	0.14	0.16	0.15	0.15	0.16	0.14	0.14	0.14	0.11
MgO	7.41	7.26	7.44	7.78	7.38	7.56	4.25	6.99	6.60	7.15	6.46	5.96	5.07
CaO	8.41	8.33	8.33	8.06	7.70	8.09	8.64	7.71	7.84	7.68	7.02	6.68	5.90
Na_2O	4.10	3.94	3.99	3.75	3.45	3.79	4.33	3.99	4.08	4.28	4.94	5.97	5.68
K_2O	1.48	1.49	1.58	2.15	1.23	1.57	1.71	1.62	0.99	2.02	3.25	2.96	2.77
P_2O_5	0.45	0.44	0.61	0.64	0.46	0.50	0.57	0.53	0.33	0.73	1.29	1.83	0.92
Total	100.36	100.56	99.98	99.85	97.35	100.41	100.00	100.26	100.51	98.17	98.86	98.45	99.14
Na_2O+K_2O	5.58	5.43	5.58	5.90	4.68	5.36	6.04	5.61	5.07	6.31	8.20	8.92	8.45

Abbreviations: BSN - basanite, TRB - trachybasalt, TPH - tephrite, PHT - phonotephrite.
Locality numbers are listed in fig.5.

plateau, Derbi-, and Shivit-Taiga volcanoes are mostly trachybasalts, whereas smaller volcanoes are composed of basanites and tephrites. The compositions of lavas from each given volcano fall into the small area, however some make certain trends. For instance, the lavas of lower and upper plateau, Yurdawa and Kadyrskii volcanoes show positive correlations between silica and alkali, whereas some younger volcanoes (Ploskii, Kok-Hemskii) show oxide variations at relatively constant SiO_2 content (49-49.5%). This feature may represent increasing role of clinopyroxene in fractionation processes.

Fig. 6 shows compositional variations of major-element oxides against MgO content. With the exception of discrete volcanoes (Uyuk, Ulug-Oo, Shui), most other lavas overlap in these diagrams. Higher SiO_2, K_2O, P_2O_5 and lower Al_2O_3, CaO, TiO_2 characterize Uyuk

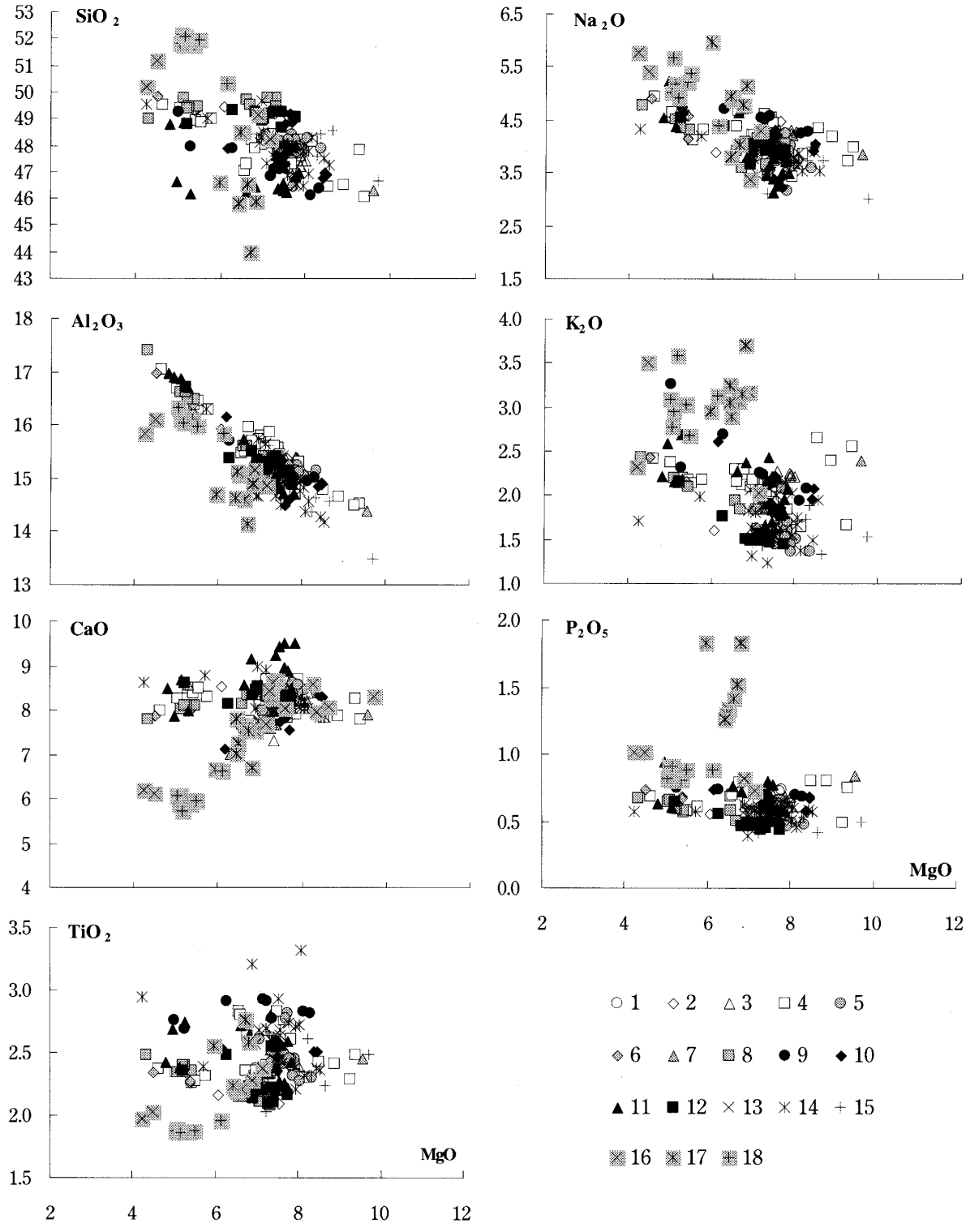

Fig.6. Major element compositions of the Tuvinian basalts. Symbols as in Fig.5.

Table 3. Trace element analyses of lavas from Azas Plateau

Locality	2	1	1	4	5	5	6	7	8	9	10	11	11
Sample No	BH-2	UA-1	UA-2	PR-2	ST-5	ST-6	KH-3	CHD-1	PL-2	YD-1	KD-1	DB-2	DB-4
Age (Ma)	Holocene	0.048	0.048	0.075	0.11	0.11	0.15	0.21	0.225	0.29	0.56	0.725	0.725
Rock type	BSN	BSN	BSN	BSN	TRB	TRB	PHT	BSN	TRB	PHT	BSN	TPH	BSN
Sc	20.2	12.8	15.8	17.1	17.0	13.4	17.4	20.4	20.9	7.2	21.8	15.6	16.8
V*	186	192	198	171	168	169	169	188	169	110	184	185	204
Cr	175	85	106	159	128	106	103	232	204	24	198	133	165
Co	45.6	44.1	43.1	38.3	45.5	40.6	30.7	52.2	43.9	33.8	50.9	40.0	42.6
Ni	252	96	93	196	93	82	140	319	201	46	265	77	66
Cu	61.5	33.1	29.9	53.7	61.2	32.5	50.9	68.7	58.5	25.5	60.1	31.5	41.8
Zn*	125	126	127	118	130	129	113	114	114	190	122	123	115
Ga	22.9	22.3	21.7	22.1	22.3	20.4	23.9	21.1	21.7	26.6	21.8	20.7	22.8
Rb	18.0	21.6	18.5	24.7	15.6	13.3	27.3	28.6	20.7	31.1	24.1	18.0	26.8
Sr	378	627	614	899	597	556	943	290	709	726	831	515	738
Zr*	221	242	240	226	181	188	244	210	202	346	214	256	229
Y	21.6	22.7	22.0	22.1	20.3	20.6	21.7	19.4	21.1	20.6	22.0	21.2	24.0
Zr	238	226	194	243	161	166	268	220	213	354	221	176	230
Nb	47.0	51.3	44.1	47.2	34.9	36.1	54.1	54.3	38.0	83.4	48.1	37.1	56.8
Cs	0.208	0.252	0.231	0.287	0.208	0.076	0.307	0.331	0.286	0.364	0.255	0.260	0.346
Ba	339	337	320	376	265	281	448	468	321	387	340	294	407
La	28.3	26.8	23.3	28.1	18.7	20.3	31.9	31.4	24.2	33.5	27.0	19.9	31.0
Ce	58.6	56.9	50.2	60.0	39.8	43.3	65.1	68.0	50.4	70.2	58.8	41.3	65.6
Pr	7.43	7.05	6.40	7.77	5.24	5.67	7.97	8.21	6.32	8.47	7.05	5.31	8.19
Nd	30.7	29.8	28.1	33.1	23.6	25.3	27.9	34.6	26.6	35.3	30.2	23.8	35.4
Sm	6.82	6.64	6.23	7.34	5.32	5.89	7.08	7.23	6.09	7.39	6.55	5.41	7.67
Eu	2.23	2.12	2.05	2.41	1.97	2.01	2.28	2.27	1.94	2.46	2.20	1.84	2.44
Gd	6.94	6.22	5.94	9.60	5.27	5.64	7.19	7.28	6.13	7.07	6.61	5.36	7.06
Tb	0.97	0.95	0.91	1.01	0.85	0.92	0.97	0.93	0.87	1.03	0.93	0.81	1.04
Dy	5.28	4.76	4.66	5.45	4.48	4.62	5.04	4.79	4.77	5.01	5.03	4.51	5.14
Ho	0.97	0.88	0.87	1.00	0.81	0.87	0.93	0.85	0.87	0.83	0.92	0.87	0.95
Er	2.52	2.17	1.95	2.65	1.80	2.01	2.43	2.22	2.36	1.84	2.36	1.96	2.28
Tm	0.32	0.29	0.28	0.34	0.26	0.30	0.32	0.27	0.31	0.25	0.31	0.29	0.31
Yb	1.58	1.48	1.58	1.65	1.40	1.52	1.51	1.21	1.58	1.28	1.54	1.52	1.68
Lu	0.25	0.21	0.21	0.26	0.19	0.21	0.24	0.20	0.24	0.16	0.24	0.24	0.24
Hf	5.50	4.91	4.18	5.38	3.79	4.00	5.83	5.08	4.93	7.25	5.20	4.00	5.06
Ta	2.96	3.44	2.80	3.01	2.07	2.18	3.08	3.15	2.32	5.00	2.97	2.27	3.45
Pb*	0.9	n.d.	n.d.	0.2	n.d.	0.2	n.d.	0.2	0.8	3.9	1.0	n.d.	n.d.
Th	2.75	2.49	2.17	2.90	1.65	1.82	3.12	2.92	2.36	3.55	2.66	2.00	3.00
U	0.99	0.90	0.80	1.03	0.46	0.60	1.06	0.92	0.73	1.26	0.98	0.80	1.07
Ce/Sm	8.59	8.57	8.06	8.17	7.48	7.35	9.19	9.41	8.28	9.50	8.98	7.63	8.55
Zr/Hf	43.3	46.0	46.4	45.2	42.5	41.5	46.0	43.3	43.2	48.8	42.5	44.0	45.5
Nb/Ta	15.9	14.9	15.8	15.7	16.9	16.6	17.6	17.2	16.4	16.7	16.2	16.3	16.5
Ba/Rb	18.8	15.6	17.3	15.2	17.0	21.1	16.4	16.4	15.5	12.4	14.1	16.3	15.2
Th/U	2.77	2.78	2.72	2.82	3.57	3.02	2.94	3.18	3.25	2.82	2.71	2.50	2.80

Analyses were performed by ICP-MS in Akita University except those marked with star representing XRF in Hirosaki University

Table 3. (continued)

Locality	15	15	13	14	14	14	14	14	15	16	17	17	18
Sample No	BH-3	BH-4	SB02	UP-1	UP-2	UP-3	UP-4	UP-5	LP-1	SB08	SB13	SB16	SB17
Age (Ma)	2.1	2.1		1.65	1.65	1.65	1.65	1.65	1.73	23	23	23	28
Rock type	TRB	TRB	TRB	BSN	TRB	TRB	TRB	TRB	TRB	BSN	PHT	PHT	PHT
Sc	6.6	6.5	20.4	7.8	9.8	6.0	16.8	13.5	17.8	19.6	14.6	12.3	--
V*	150	--	174	--	--	--	240	--	170	147	134	131	127
Cr	92	170	203	102	141	104	86	89	131	170	169	143	108
Co	36.7	38.4	46.8	42.3	37.7	40.8	27.3	41.1	41.5	42.4	37.3	37.3	--
Ni	89	92	222	104	84	94	29	78	82	209	261	269	34
Cu	27.1	56.4	62.1	37.2	37.4	51.2	31.5	32.3	59.8	67.1	79.0	76.2	23.6
Zn*	250	--	131	--	--	--	210	--	180	127	132	146	123
Ga	16.8	20.7	23.0	22.3	21.4	20.3	23.2	23.0	23.5	21.6	23.2	25.7	--
Rb	7.1	7.2	17.6	12.7	6.0	7.7	19.3	18.4	10.3	33.1	38.0	30.3	32.4
Sr	414	466	697	559	356	444	519	532	377	824	1420	1820	1229
Zr*	146	139	201	203	144	171	205	183	138	211	317	360	--
Y	17.4	19.0	22.6	19.8	18.9	19.1	25.3	22.8	23.5	22.7	23.9	28.0	22.5
Zr	139	166	204	232	167	188	221	205	162	208	344	396	282
Nb	27.8	32.2	39.3	55.0	35.4	41.5	46.8	43.0	26.6	71.6	110.0	142.0	66.7
Cs	0.061	0.055	0.106	0.078	0.014	0.055	0.207	0.205	0.150	0.496	0.792	0.836	--
Ba	246	268	282	321	201	219	256	255	176	420	530	609	579
La	15.9	18.1	25.0	25.3	15.6	18.7	23.0	22.0	12.8	29.1	58.6	78.7	--
Ce	35.9	37.5	55.1	52.4	34.6	40.1	49.3	47.0	27.9	59.7	106.0	145.0	69.7
Pr	4.53	5.03	7.01	6.76	4.53	5.34	6.47	6.20	3.67	7.37	12.90	17.40	--
Nd	19.5	21.2	30.2	29.9	21.3	23.9	29.2	26.9	17.6	30.7	50.5	66.3	31.5
Sm	4.80	4.77	6.88	6.56	5.23	5.83	6.87	6.24	4.85	7.09	9.54	12.50	--
Eu	1.51	1.77	2.24	2.14	1.82	1.95	2.27	2.24	1.81	2.22	2.88	3.66	--
Gd	4.53	5.07	6.79	6.06	5.17	5.59	6.60	5.97	5.34	7.02	9.47	10.00	--
Tb	0.75	0.74	0.90	0.88	0.82	0.90	1.07	0.94	0.91	0.91	1.17	1.32	--
Dy	3.73	3.87	5.32	4.46	4.26	4.49	5.35	4.90	4.81	5.40	5.88	6.89	--
Ho	0.70	0.69	0.97	0.75	0.74	0.79	0.97	0.93	0.88	0.99	1.02	1.15	--
Er	1.73	1.82	2.38	1.90	1.80	2.01	2.35	1.98	2.20	2.45	2.70	2.73	--
Tm	0.22	0.24	0.33	0.22	0.25	0.24	0.33	0.30	0.30	0.31	0.31	0.32	--
Yb	1.38	1.41	1.63	1.31	1.38	1.40	1.78	1.66	1.53	1.55	1.24	1.02	--
Lu	0.18	0.20	0.24	0.20	0.18	0.19	0.25	0.21	0.23	0.24	0.22	0.19	--
Hf	3.47	3.44	5.48	4.92	3.59	4.22	5.03	4.63	3.80	5.41	7.46	8.54	--
Ta	1.75	1.84	2.77	3.34	2.26	2.68	2.66	2.57	1.75	4.54	6.56	8.18	--
Pb*	4.9	--	n.d.	--	--	--	2.5	--	1.9	n.d.	2.2	n.d.	2.4
Th	1.16	1.37	2.45	1.96	1.20	1.34	2.13	2.08	1.43	3.66	6.46	8.02	4.00
U	0.55	0.54	0.69	0.75	0.57	0.60	0.65	0.72	0.39	1.21	2.21	2.54	--
Ce/Sm	7.48	7.86	8.01	7.99	6.62	6.88	7.18	7.53	5.75	8.42	11.11	11.60	--
Zr/Hf	40.1	48.3	37.2	47.2	46.5	44.5	43.9	44.3	42.6	38.4	46.1	46.4	--
Nb/Ta	15.9	17.5	14.2	16.5	15.7	15.5	17.6	16.7	15.2	15.8	16.8	17.4	--
Ba/Rb	34.7	37.1	16.0	25.3	33.7	28.5	13.3	13.9	17.1	12.7	13.9	20.1	17.9
Th/U	2.11	2.55	3.56	2.60	2.10	2.23	3.28	2.87	3.66	3.02	2.92	3.16	--

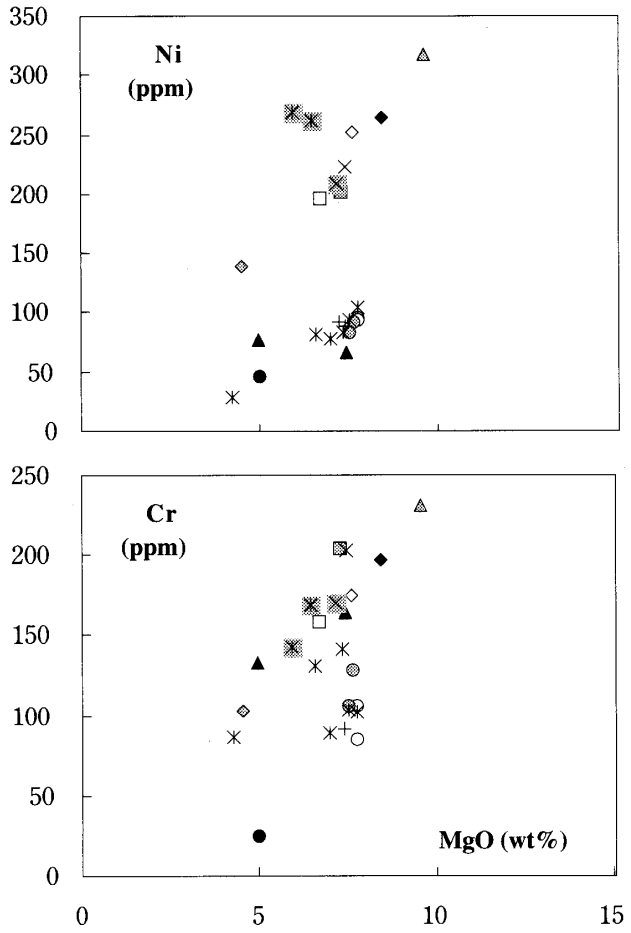

Fig.7. Variations of Ni and Cr abundances with MgO in the Tuvinian Cenozoic basalts. Symbols as in Fig.5.

and Shui basalts at a given MgO concentration. For major trends, although the data show some scatter, the following correlations are evident: SiO_2, Al_2O_3, alkali increase, whilst CaO, TiO_2, P_2O_5 do not change significantly with decreasing MgO content in these basalts.

Ni and Cr abundances are highly variable: Ni ranges from 28.5 to 319 ppm (Fig. 7) and Cr from 24.4 to 232 ppm. The most magnesian basalts have Ni contents close to those of primary basalts: relatively low MgO content (less than 10% with average 6-8%) may result from olivine fractionation. Basalt lavas from some localities bear pyroxenite, olivine pyroxenite, and wehrlite xenoliths, which represent the products of deep crystallization. Also, some basalts contain various amounts of clinopyroxene, ilmenite-titanomagnetite and sanidine megacrysts which have been crystallized during the ascent of melt to the surface.

Table 3 lists the REE and other trace-element abundances. Chondrite-normalized REE patterns are shown in Fig. 8. The REE compositions of Tuvinian lavas are similar to those of other alkaline basalts from the similar tectonic settings. The enrichment of LREE contents correlates with the volume of erupted materials; id est. it is possibly controlled by the degree of partial melting. This feature is regular, so that we can qualitatively estimate the volume of products from each eruptive stage. Despite the significant destruction of the volcanic edifice

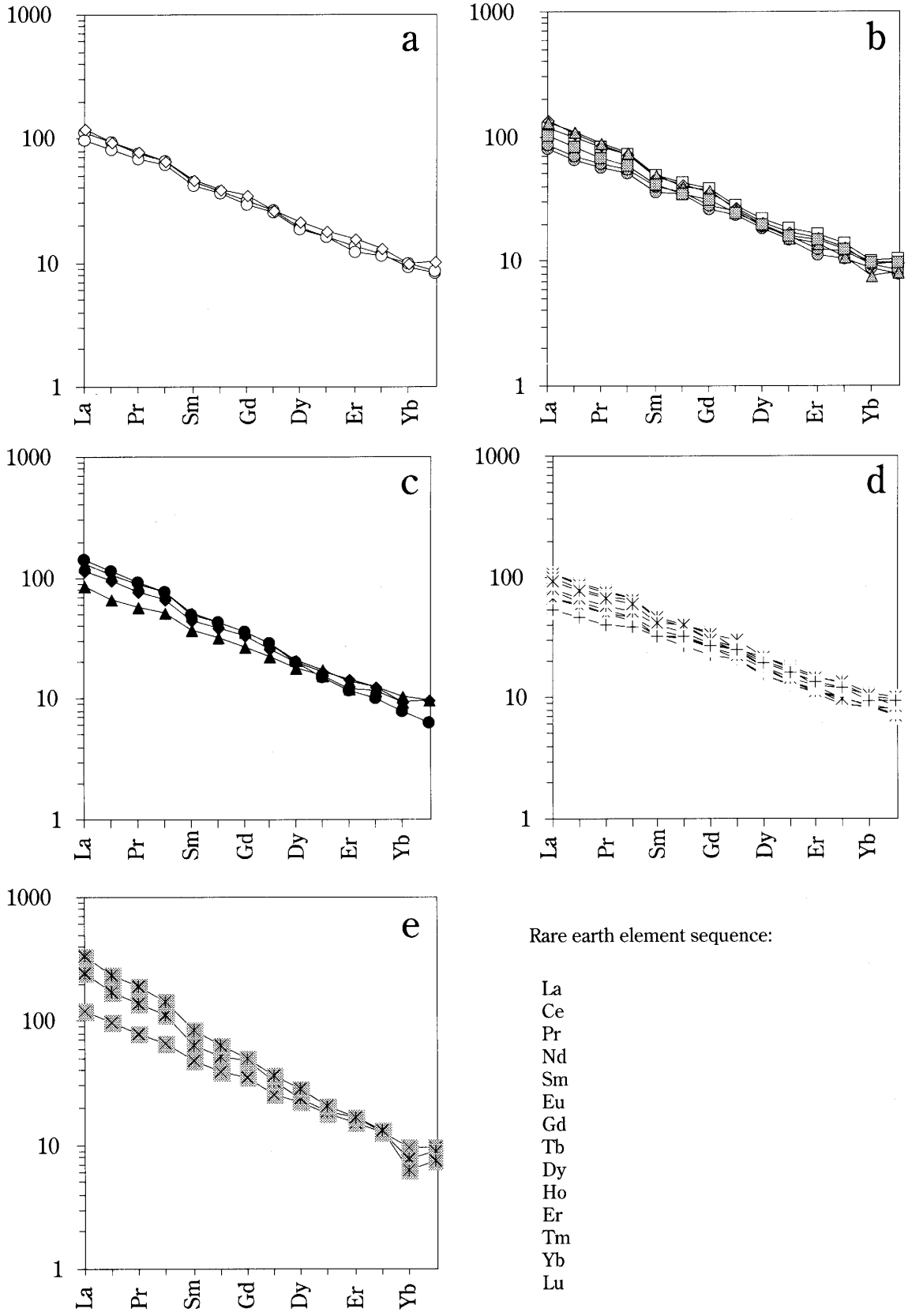

Fig.8. Chondrite-normalized REE abundance patterns for the Tuvinian Cenozoic basalts: a - Holocene-0.05Ma volcanoes; b - 0.075-0.225Ma volcanoes; c - 0.29-0.76Ma volcanoes; d - 1.2-2.1Ma lava flows; e - 23-28Ma discrete volcanoes. Normalization values after McDonough, Sun (1995). Symbols as in Fig.5.

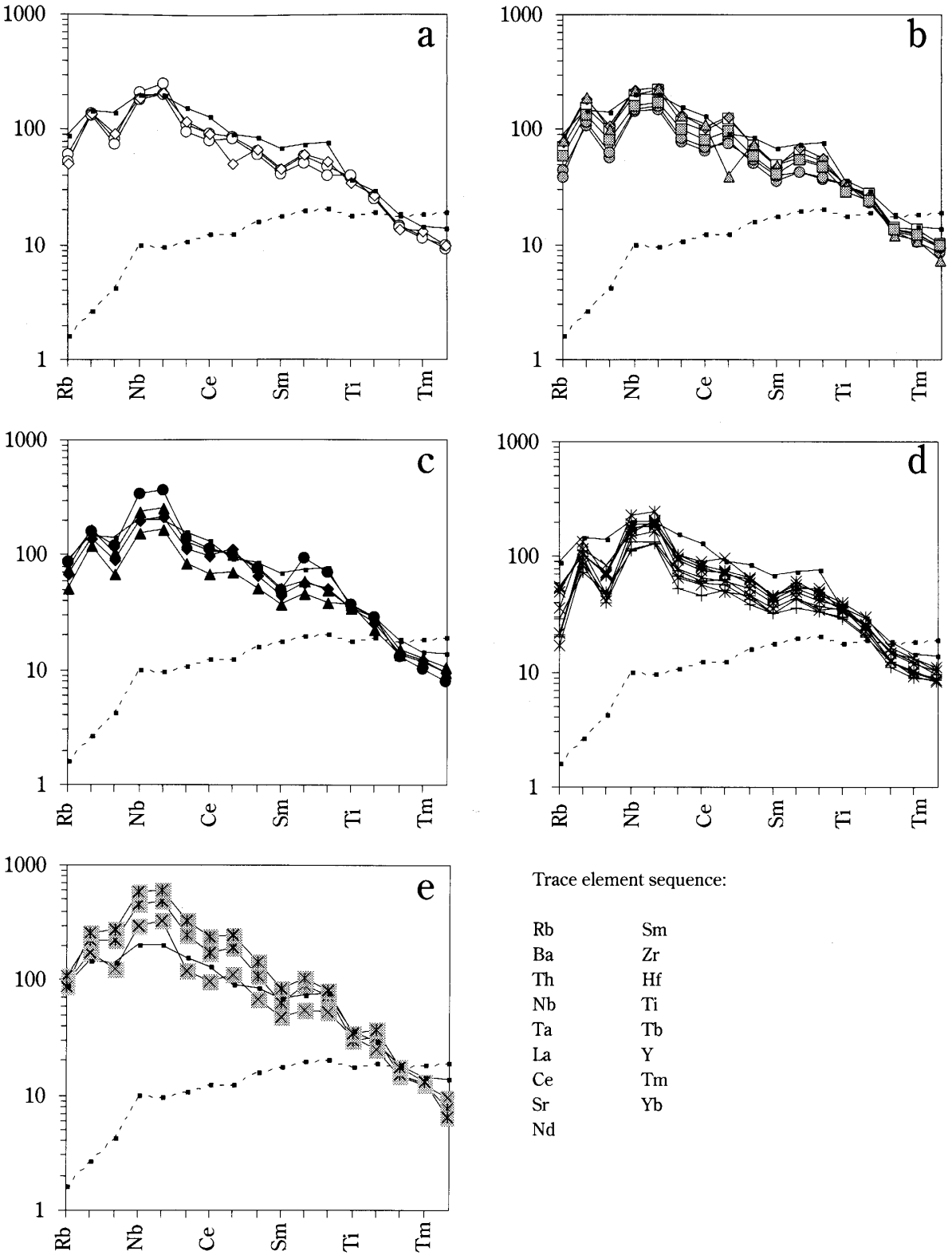

Fig.9. Chondrite-normalized trace-element abundances in the Tuvinian Cenozoic basalts. Solid line - mean OIB; dashed line - N-MORB. Symbols as in Figs.5,8.

by glaciers and other erosional processes, the most voluminous were the volcanic products from the lower and upper plateau units. Certain REE patterns have a slight Yb trough, which may imply the origin of these magmas from the garnet-bearing source. Characteristic variations of the REE patterns (Fig. 8) are as follows:

(1) Light REE (LREE) are enriched relative to heavy REE (HREE). In most cases, the ratios between chondrite-normalized values, $(La/Lu)_N$=11-22; the lowest $(La/Lu)_N$ was found for the lower plateau basalts (5.8-9.6) and the highest ratio, for basanites of the Ulug-Oo Volcano (27.9-43.9);
(2) HREE's are constant relative to LREE's both in absolute and relative terms;
(3) Negative Eu anomalies are absent;
(4) Most basalts have a slight Sm inflection. Enrichment of Nd relative to Sm is characteristically found for EM1 mantle source.

Abundances of the other trace elements are arranged from left to right with increasing compatibility and normalized to chondritic values (Fig. 9). The spectrum of trace element patterns is similar to that of OIB-like source. In general, the plateau basalts are depleted relative to OIB in all the trace elements except lavas of smaller volcanoes and lavas of discrete volcanic centers. The uniqueness of lava composition is relative enrichment in Ba, Nb, Ta, Zr and depletion in Th. The Nb-Ta enrichment is typically found for HIMU ocean island basalts, such as Bouvet, St.Helena, and Ascension, however it is even higher in the Azas basalts. The Ulug-Oo Volcano has the most enriched trace element patterns. Despite its discrete location, it has similar anomalously high Nb-Ta content and slight Th depletion.

Highly incompatible element ratios mostly do not vary systematically with Th abundances, which vary by a factor of 8 (Fig. 10). It suggests that, except basalts of lower and upper plateau units, these ratios are not considerably affected by partial melting and crystallization processes, and represent the ratios of the mantle sources. The lower and upper plateau basalts have lower Rb/Nb, Th/Nb, and Th/U ratios than the rest. Characteristics of all the Azas basalts are high Zr/Hf ratios, varying from 37 to 49, contrasting to uniform values for most terrestrial basalts (about 36-37).

6. Petrogenesis

With the exception of local volcanic activity started 28 Ma ago as small discrete volcanic centers; the major activity started 14-16 Ma ago. The lava flow fragments are widely distributed all over NE Tuva and occur at different altitudes. Their alignments along paleovalleys suggest their formation as valley-filling extended lava flows effused before recent tectonic movement and subsequent erosion. There are no volcanic products having ages between 14 and 2.1 Ma. Starting 2.1 Ma ago until present, there has been no regressive tendency in volcanism. The alignment of volcanic centers seems to reflect the presence of deep-seated tectonic fissure. In some cases, the eruptions occurred in the intersections of fissures and deep river valleys at lower altitudes (Bii-Khemskii Volcano), however more than half volcanoes makes a single lineament in the SW-NE direction (Sagan, Derbi-Taiga, Yurdawa, Shivit-Taiga, Kadyrskii, Sorug-Chushku-Uzu). Further to the NE in this direction two more volcanoes fit this alignment (Kropotkin and Peretolchin). The volume estimation

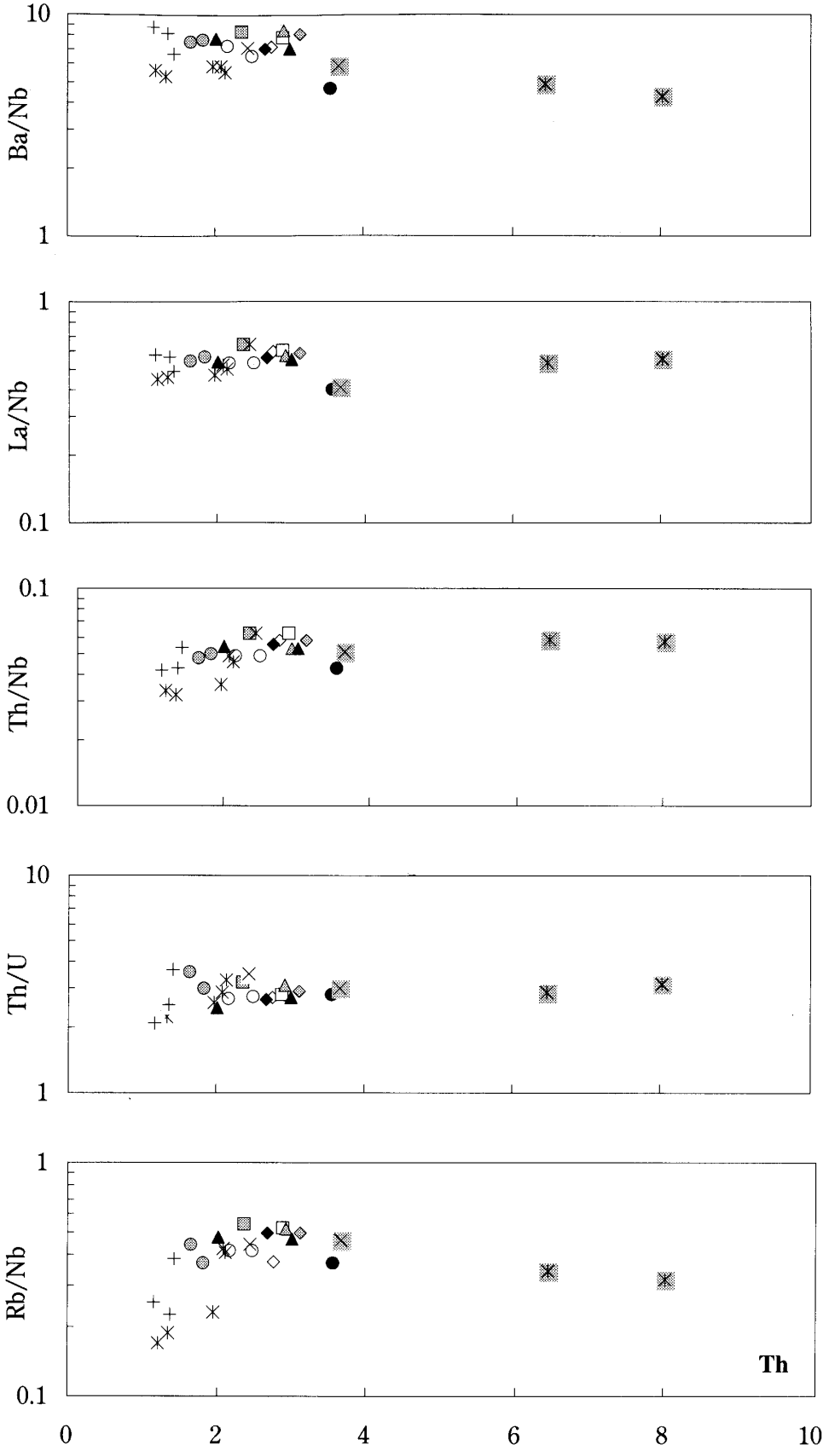

Fig.10. Variations of trace-element ratios with Th abundances in the Tuvinian Cenozoic basalts. Symbols as in Fig.5.

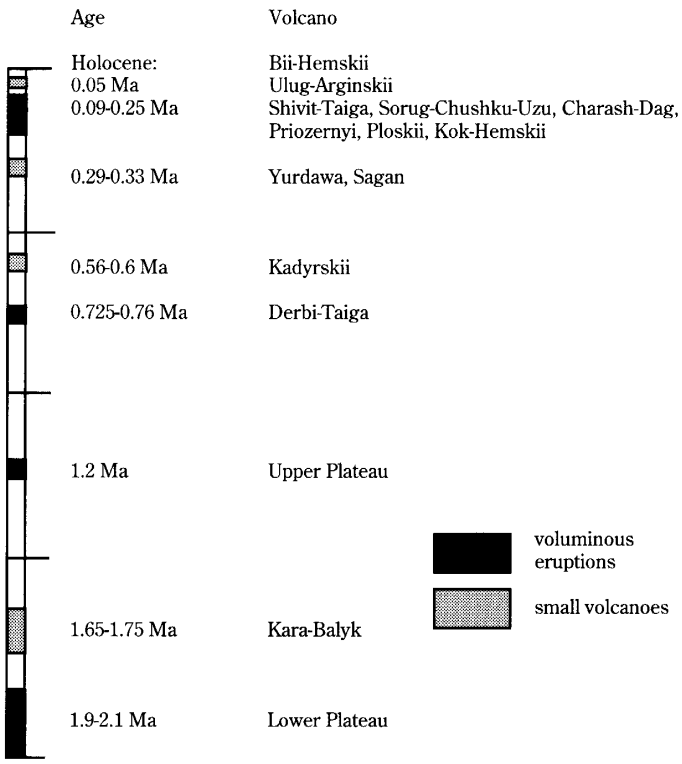

Fig.11. Time scale of eruptive stages showing a periodicity of voluminous eruptions.

of erupted products is difficult, because of significant erosion by contemporaneous or later glaciers. Voluminous eruptions are found with a period of 450-550 thousand years; occurrence of small volcanoes between them is scarce and irregular (Fig. 11).

Resemblance in chemical compositions is thought to result principally from uniformity of mantle source, whereas observed differences are considered to be a matter of partial melting degree and fractional crystallization. Narrow range of silica contents (46-50 wt.% for the majority) allows suggesting about the same depth of origin, because in basaltic melts it is mainly controlled by pressure [Takahashi and Kushiro 1983: 859-879; McKenzie and Bickle 1988: 625-679]. Fractional crystallization does not change it significantly, unless the process goes too far [Wright and Fiske 1971: 1-65]. Definitely, H_2O and CO_2 contents in source may control melt compositions, for instance, H_2O affects silica enrichment, whereas the presence of CO_2 increases alkaline affinities of melts [Eggler 1973: 491-495]. Indeed, the presence of H_2O and CO_2 was detected for some other localities of the Baikal Rift [Ionov et al. 1993: 1141-1175; Litasov and Litasov 1999a: 667-670; 1999b: 663-666] due to the presence of hydrous minerals in mantle-derived peridotites and comagmatic cumulative xenoliths. However, there was no sign found for hydration of mantle beneath the Azas Plateau (except extremely rare amphibole bearing cumulates found in a single locality Hoogzhu-Taiga). As well, the effects of volatile components are probably negligible due to their low solubility and definite undersaturation. Therefore, observed variations of REE and other trace elements have to be mostly controlled by degree of partial melting.

The rate of partial melting was examined using Th-Cr log-log diagram (Fig. 12)

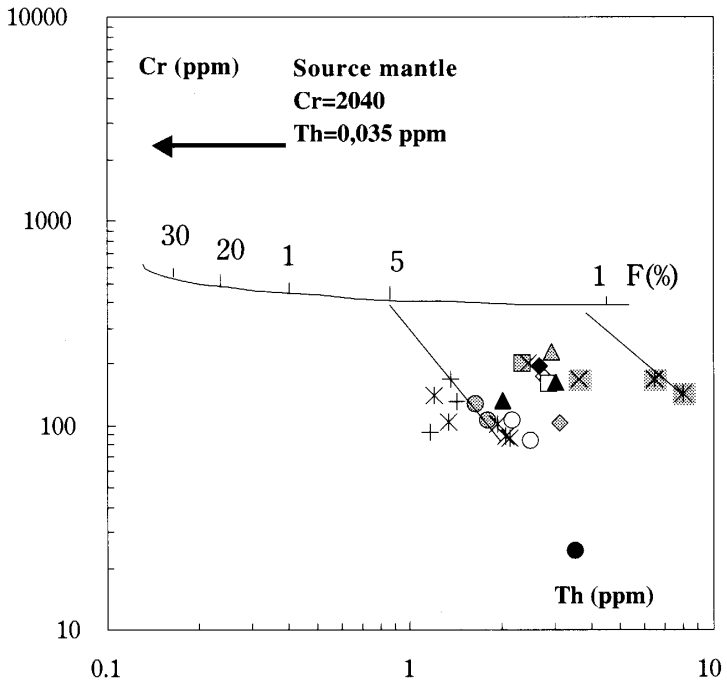

Fig.12. Th-Cr log-log diagram showing modeled partial melting of peridotite mantle source.

which showed the degree of melting varying from 1 to 7 %. Consistently with the above assumptions, the most voluminous eruption source undergone 4-7 % melting degree, whereas a majority of smaller volcanoes has been formed by 1.5-2 % of source partial melting.

Testing fractional crystallization effect showed for the most trends olivine fractionation from the beginning and addition of clinopyroxene and feldspar at final fractionation stages. However, fractionation didn't change significantly geochemical features of studied rocks. Even the rocks including feldspar megacrysts do not have any Eu troughs. Thus, we may exclude fractionation as potential mechanism in changing rock trace chemistry.

We compared Azas alkaline basalts with those from the other world regions and different tectonic settings. The last included potassic Northeast China basalts [Zhang et al. 1995: 1275-1303], Hawaiian alkaline basalts [Chen et al. 1990: 197-218], Cameroon volcanic line [Marzoli et al. 2000: 87-109], which straddles the African continental margin, Main Ethiopian Rift, Fort Selkirk (Yukon, Canada), Cantal volcano of Massif Central (France). In compilation diagrams, we also used trace element data for the minerals of mantle-derived and cumulate xenoliths found in the Azas basalts.

The range of REE and trace element patterns is shown on the OIB-normalized diagrams (Fig. 13). The Azas lava plateau basalts are generally depleted in the most REE and trace elements, whereas lavas of smaller volcanoes are closer or exceeding some OIB values. Both are definitely depleted in HREE. Similar peculiarities are characteristic for the Udokan plateau. High LREE enrichment is characteristic for Northeast China, less enriched are lavas from Yukon, Canada, and Massif Central. Cameroon Line and Hawaiian alkaline basalts fit

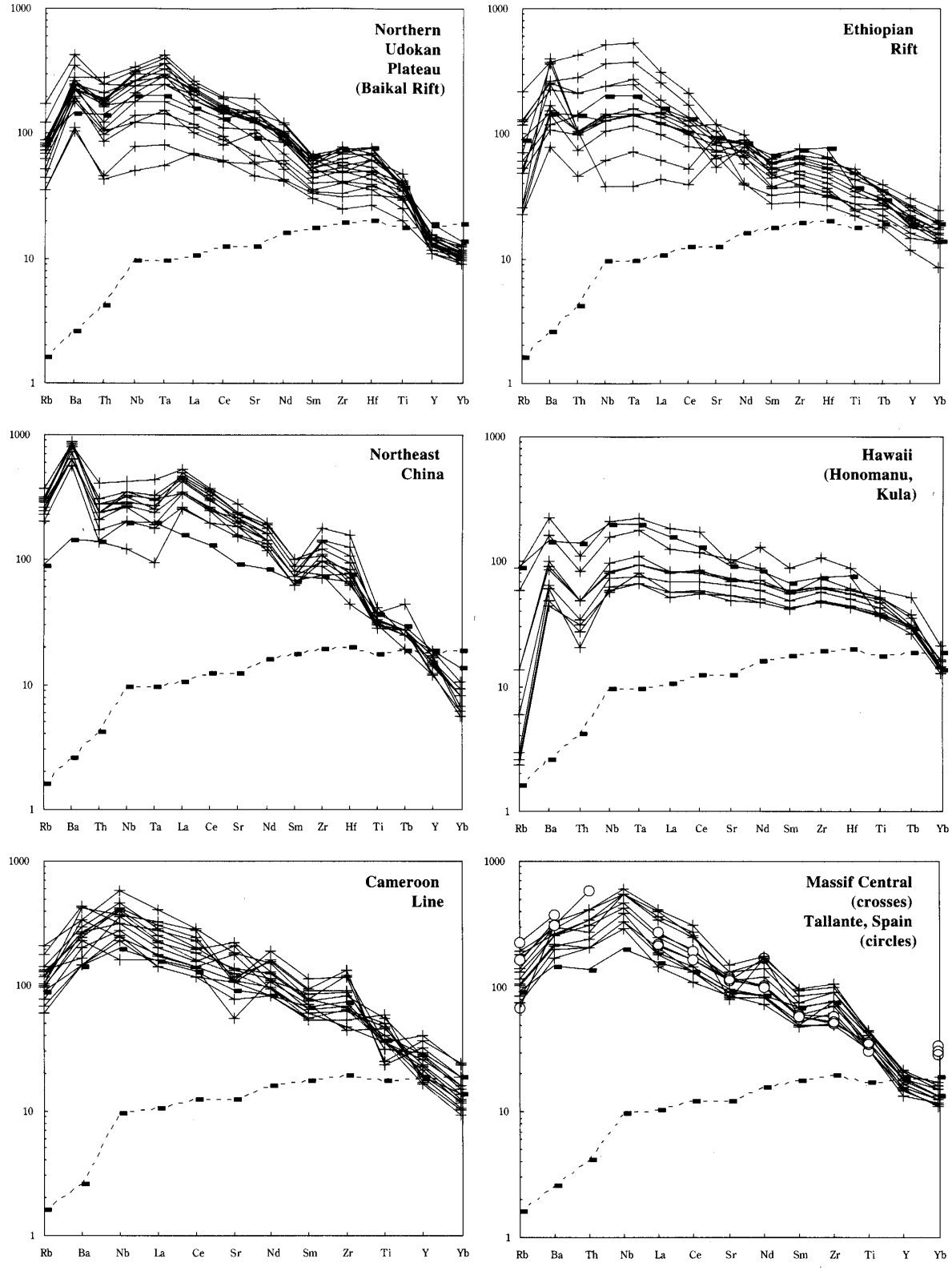

Fig.13. Comparison of basalt compositions from different localities of rift-related tectonic settings. The vertical axis, solid line, dashed line, as in Fig.9.

the mean OIB, whereas Ethiopian Rift transitional basalts are definitely depleted in LREE and enriched in HREE.

Great discrepancy between above regions begins when we start comparing trace element ratios, even those, which are expected to be about constant in different settings. The Zr/Hf ratio for the Azas basalts, after Dupuy et al. (1992), may be explained by involving garnet in partial melting, of which D_{Zr} and D_{Hf} may differ two times under the pressure about 25 kb (Hauri et al., 1994). Farther increasing in this ratio was explained by metasomatism (CO_2-rich fluids). La/Sm ratio increases with decreasing melt fraction. The upper mantle is obviously heterogeneous in Nb/Ta ratio; this may reflect its discrepancy in the rocks of even one region. Again, if in cpx the partition coefficients between Nb and Ta are compatible, it is an order difference for the garnet. However, the partition coefficients between source minerals and melt can not explain greater differences between trace element ratios. Besides the influence of metasomatizing fluids on element ratios is not encompassed sufficiently, it is likely to involve metasomatic agents into generation of alkaline basalt melts. For example, the appearance of pargasitic amphibole in some Azas cumulates is indirect evidence for such an influence.

General Nb-Ta enrichment observed in the Azas plateau basalts was found in several other world localities and it is an evidence for the presence of HIMU component, which is representative of recycled lithosphere.

7. Conclusions

The Azas Plateau is composed mostly of trachybasalts-basanites, as it was described for the other Baikal Rift Zone localities. The basalts are silica undersaturated except a few hypersthene normative lower and upper plateau basalts.

The textures of volcanic rocks are quite uniform suggesting for resemblance of melt evolution, fractionation and crystallization paths. However, local varieties were detected for certain volcanoes, such as the Derbi-Taiga Volcano with abundant Ti-augite phenocrysts, the Sagan Volcano lavas filled with olivine phenocrysts, Early Pleistocene lavas with numerous megacryst assemblages, etc.

Despite of mentioned above uniformity, major element compositions reveal variously oriented trends for each given volcano suggesting for different crystal fractionation paths.

Discrete volcanoes and lava flows off the Azas Plateau have higher alkalinity and show enrichment in REE and other incompatible elements.

Certain lavas have high Ni and Cr contents allowing suggestion for some melts to be close to primary compositions. However, low Mg contents request early olivine fractionation even for the most primitive melts.

REE and trace element spidergram patterns, together with melting degree modeling, reflect various degrees of partial melting of primitive to slightly depleted mantle substrate varying from less than 1 to 5-7% of partial melting.

Trace element composition reflects a complicity of mantle source having some features characteristic for EM1 and HIMU components. The first represents underlying upper mantle and reflects probable decompressional melting under extensional conditions. The second is

representative of recycled lithosphere and evidences for a presence of plume component.

Acknowledgements

The authors acknowledge Prof. T. Yoshida of Tohoku University for review comments, and Prof. A. Isobe of CNEAS, Tohoku University for his kind editorial handling of this paper. Prof. T. Mizuta and Dr. D. Ishiyama of Akita University kindly provided us the opportunity to use their ICP-MS facility, and Ms. H. Satoh helped us sample preparations and measurements. We owe high-precision data to their laboratory, which is efficiently organized and well maintained by the helpful staff willing to support. The first author (Y. L.) expresses his gratitude to RIMR, Akita University for nine months visiting period to accomplish this study. The work was also supported by Russian Foundation for Basic Research, grant #01-05-65322.

References

Adamovich, A.F., Grossvald, M.G. and Zonenshain, L.P. 1959

New data on the Kropotkin and Peretolchin volcanoes. In: *Materials of Regional Geol., Proc. Of the All-Union Aerogeological Trust 5,* Moscow: Gosgeoltechizdat (In Russian).

Baratov, R.B., Lutkov, V.S., Sharapov, N.V. and Kabanova L.K. 1988

To the composition of the South-Gissar zone upper mantle (Southern Tien-Shan). *Doklady Akademii Nauk* 299, 3, Moscow: Russian Academy of Sciences.

Chen, C.-Y., Frey, F.A. and Garcia, M.O. 1990

Evolution of alkalic lavas at Haleakala Volcano, east Maui, Hawaii. *Contrib. Mineral. Petrol.* 105, Berlin: Springer-Verlag.

Devirts A.L., Rasskazov S.V., Polyakov, A.I. and Dobkina E.I. 1981

Radiogenic carbon dating for the young volcanoes of the Udokan Range (Northeast Pribaikalie). *Geokhimiya* 8, Moscow: Acad. Sci. USSR Publ.

Dobretsov N.L., Zagruzina I.A. 1977

To the peculiarities of modern basaltic magmatism at the estern part of Tien-Shan. Proceedings of the USSR Acad. Sci. 235, 3, p. 648-651 (in Russian)

Dupuy C., Liotard J.M., Dostal J. (1992)

Zr/Hf fractionation in intraplate basaltic rocks: carbonate metasomatism in the mantle source. Geochimica et Cosmochimica Acta, v. 56, p. 2417-2423.

Eggler, D.H. 1973

Principles of melting of hydrous phases in silicate melt. In: *Annual Report of Geophys. Lab.,* Year Book 72, Washington: Carnegie Institute.

Grosvald, M.G., Stankevich, E.N. and Uflyand, A.K. 1959

New data on the basalts of Kamsara-Biikhem river basin, Northeast Tuva. In: *Materials of regional geology, Proceedings of the All-Union Aerogeological Trust, Issue* 5, Moscow: Gosgeoltechizdat (In Russian).

Hauri E.H., Wagner T.P., Grove T.L. (1994)

Experimental and natural partitioning of Th, U, Pb, and other trace elements between garnet, clinopyroxene and basaltic melts. Chemical Geology, v. 117, p. 149-166.

Hirano, N. 2000

Discovery of 6-8 Ma alkaline basalt from the oceanward slope toe of the Japan Trench. *Eos Trans. AGU* 81, 22, Western Pacific Geophys. Meet. Suppl., Tokyo: American Geophysical Union.

Hole, M. J., Kempton, P. D. and Millar, I. L. 1993
Trace-element and isotopic characteristics of small-degree melts of the asthenosphere: Evidence from the alkalic basalts of the Antarctic Peninsula. *Chemical Geol.* 109, Amsterdam: Elsevier.

Ionov, D.A., Ashchepkov, I.V., Stoşch, H.-G., Witt-Eickshen, G., and Seck H.A. 1993
Garnet peridotite xenoliths from the Vitim volcanic field, Baikal region: the nature of the garnet-spinel peridotite transition zone in the continental mantle. J. Petrol. 34, 6, Oxford University Press.

Keen, C.E., Courtney, R.C., Dehler, S.A. and Williamson, M.-C. 1994
Decompression melting at rifted margins: comparison of model predictions with the distribution of igneous rocks on the eastern Canadian margin. *Earth Planet. Sci. Lett.* 121, Amsterdam: Elsevier.

Litasov, Yu.D. and Litasov, K.D. 1999a
Mantle geotherms of different ages as an evidence for thinning of continental lithospheric mantle during rifting. Doklady Akademii Nauk 365, 5, Moscow: MAIK Nauka.

———— 1999b
Reactional modification of primitive mantle recorded in mantle xenoliths from alkaline basalts of the Vitim Plateau. Doklady Akademii Nauk 368, 5, Moscow: MAIK Nauka.

Logachev, N.A. and Zorin, Y.A. 1987
Evidence and causes of the two-stage development of the Baikal Rift. Tectonophysics 143, Amsterdam: Elsevier.

Lutkov V.S., Sharapov N.V., Gopfauph L.M. (1988)
Petrochemical types of alkaline basaltoides from the southern Tien-Shan. Proceedings of the USSR Acad. Sci., v.303, No 5, p. 1221-1226 (in Russian)

Marzoli, A., Piccirillo, E.M., Renne, P.R., Bellieni, G., Iacumin, M., Nyobe, J.B. and Tongwa, A.T. 2000
The Cameroon Volcanic Line revisited: petrogenesis of continental basaltic magmas from lithospheric and asthenospheric mantle sources. J. Petrol. 41, 1, Oxford University Press.

McKenzie, D. and Bickle, M.J. 1988
The volume and composition of melt generated by extension of the lithosphere. *J. Petrol.* 29, Oxford University Press.

Obruchev, S.V. 1949
Tectonics of western part of the Sayan-Baikal Caledonian Fold Belt. *Doklady Akademii Nauk* 68, 5, Moscow: Russian Academy of Sciences.

———— 1950
Modern movements and basalt eruptions of the Sayan-Tuvinian Highland. *Zemlevedenie* 43, 3, Moscow: Russian Academy of Sciences.

Rasskazov, S.V., Maslovskaya, M.N., Batyrmurzaev, A.S., Matsera, A.V., Zelenkov, P.Ya.,

Avdeev, V.A., Omarova, M.R., Gargatsev, I.O., and Magomedov, Sh.A. 1989
Composition, Sr isotopy and K-Ar dating of the modern basalts from Tuva. *Geologiya i Geophizika* 2, Novosibirsk: Nauka (In Russian).

Rasskazov, S.V., Ivanov, A.V., Bogdanov, G.V. and Medvedeva, T.I. 1994
Composition of orthopyroxenes and classification of deep-seated inclusions from the lavas of the Upper-Oka and Tuva segments of the Baikal Rift System. *Doklady Akademii Nauk* 338, 5, Moscow: Russian Academy of Sciences.

Rasskazov, S.V., Logachev, N.A., Brandt, I.S., Brandt, S.B., Ivanov, A.V., Demonterova, E.I. and Smagunova, M.A. 2000
Pulse migration of Quaternary volcanism on the East Tuvinian field. Doklady Akademii Nauk 373, 5, Moscow: MAIK Nauka.

Sasaki, M. 1999
Major element analysis of rock samples by X-ray fluorescence spectrometry. Bull. Fac. Sci. Tech. Hirosaki Univ. 1, 141-149.

Satoh, H., Ishiyama, D., Mizuta, T. and Ishikawa, Y. 1999
Rare earth element analysis of rock and thermal water samples using inductively coupled plasma mass spectrometry (ICP-MS). Sci. Tech. Rep. Fac. Eng. Resour. Sci. Akita Univ. 20, 1-8.

Stupak, F.M. 1987
Cenozoic volcanism of the Udokan Ridge. Novosibirsk: Nauka.

Takahashi, E. and Kushiro, I. 1983
Melting of a dry peridotite at high pressures and basalt magma genesis. *American Mineralogist* 68, .

Whitford-Stark, J. L. 1983
Cenozoic volcanic and petrochemical provinces of Mainland Asia. *J. Volcanol. Geotherm. Res.* 19, Amsterdam: Elsevier.

Wright, T.L. and Fiske, R.S. 1971
Origin of the differentiated and hybrid lavas of Kilauea volcano, Hawaii. *J. Petrol.* 12, Oxford University Press.

Yarmolyuk, V.V. and Kovalenko, V.I. 1990
The South-Baikal mantle hot spot and its role in formation of the Baikal Rift Zone. *Doklady Akademii Nauk* 312, 1, Moscow: Russian Academy of Sciences.

Yarmolyuk, V.V., Lebedev, V.I., Arkelyants, M.M., Prudnikov, S.G., Sugorakova, A.M., Kovalenko, V.I. 1999
Modern volcanism of the East Tuva: the chronology of volcanic events on the base of K-Ar dating. Doklady Akademii Nauk 368, 2, Moscow: MAIK Nauka.

Yarmolyuk, V.V., Lebedev, V.I., Sugorakova, A.M., Bragin, V.Yu., Litasov, Yu.D., Prudnikov, S.T., Arakelyants, M.M., Lebedev, V.A., Ivanov, V.G., Kozlovskii, A.M. 2001
East Tuvan area of modern volcanism in Central Asia: periodicity, products and character of volcanic activity. Volcanology and Seismology, 3, Moscow: MAIK Nauka.

Zhang, M., Suddaby, P., Thompson, R.N., Thirlwall, M.F. and Menzies, M.A. 1995
Potassic volcanic rocks in NE China: geochemical constraints on mantle source and magma genesis. J. Petrol. 36, 5, Oxford University Press.

Zhang, M. and O'Reilly, S.Y. 1997

Multiple sources for basaltic rocks from Dubbo, eastern Australia: geochemical evidence for plume-lithospheric mantle interaction. *Chemical Geol.* 136, Amsterdam: Elsevier.